

# Expanded CAG/CTG Repeat DNA Induces a Checkpoint Response That Impacts Cell Proliferation in *Saccharomyces cerevisiae*

Rangapriya Sundararajan, Catherine H. Freudenreich\*

Department of Biology, Tufts University, Medford, Massachusetts, United States of America

## Abstract

Repetitive DNA elements are mutational hotspots in the genome, and their instability is linked to various neurological disorders and cancers. Although it is known that expanded trinucleotide repeats can interfere with DNA replication and repair, the cellular response to these events has not been characterized. Here, we demonstrate that an expanded CAG/CTG repeat elicits a DNA damage checkpoint response in budding yeast. Using microcolony and single cell pedigree analysis, we found that cells carrying an expanded CAG repeat frequently experience protracted cell division cycles, persistent arrests, and morphological abnormalities. These phenotypes were further exacerbated by mutations in DSB repair pathways, including homologous recombination and end joining, implicating a DNA damage response. Cell cycle analysis confirmed repeat-dependent S phase delays and G2/M arrests. Furthermore, we demonstrate that the above phenotypes are due to the activation of the DNA damage checkpoint, since expanded CAG repeats induced the phosphorylation of the Rad53 checkpoint kinase in a *rad52Δ* recombination deficient mutant. Interestingly, cells mutated for the MRX complex (Mre11-Rad50-Xrs2), a central component of DSB repair which is required to repair breaks at CAG repeats, failed to elicit repeat-specific arrests, morphological defects, or Rad53 phosphorylation. We therefore conclude that damage at expanded CAG/CTG repeats is likely sensed by the MRX complex, leading to a checkpoint response. Finally, we show that repeat expansions preferentially occur in cells experiencing growth delays. Activation of DNA damage checkpoints in repeat-containing cells could contribute to the tissue degeneration observed in trinucleotide repeat expansion diseases.

**Citation:** Sundararajan R, Freudenreich CH (2011) Expanded CAG/CTG Repeat DNA Induces a Checkpoint Response That Impacts Cell Proliferation in *Saccharomyces cerevisiae*. PLoS Genet 7(3): e1001339. doi:10.1371/journal.pgen.1001339

**Editor:** Nancy Maizels, University of Washington, United States of America

**Received:** August 27, 2010; **Accepted:** February 15, 2011; **Published:** March 17, 2011

**Copyright:** © 2011 Sundararajan, Freudenreich. This is an open-access article distributed under the terms of the Creative Commons Attribution License, which permits unrestricted use, distribution, and reproduction in any medium, provided the original author and source are credited.

**Funding:** This work was supported by: National Institutes of Health grant GM063006 to CHF <http://www.nigms.nih.gov/> and a Tufts GSC Research Award to RS <http://gradstudy.tufts.edu/default.aspx>. The funders had no role in study design, data collection and analysis, decision to publish, or preparation of the manuscript.

**Competing Interests:** The authors have declared that no competing interests exist.

\* E-mail: [catherine.freudenreich@tufts.edu](mailto:catherine.freudenreich@tufts.edu)

## Introduction

Repetitive DNA is found dispersed throughout eukaryotic genomes, and in some cases is central to key biological processes such as chromosome segregation and chromosome end protection [1]. Repeat tracts are usually sites of variation among individuals, with some classes of repeats expanding to sizes that cause pathology. For example, expansion of CAG/CTG trinucleotide repeats (abbreviated CAG) have been observed to occur at several different genomic loci, causing diseases that include Huntington's disease, myotonic dystrophy, and multiple subtypes of spinal cerebellar ataxia [2-3].

CAG trinucleotide repeats are among a class of repeats that are unique in that they form hairpin secondary structures that interfere with DNA replication and DNA repair [1,4]. The repeats exhibit a threshold length beyond which expansions become increasingly likely. For CAG repeats in humans, the expansion threshold is 35–38 repeats, 100–115 bp. In addition to the instability threshold, a disease-causing threshold also exists for trinucleotide repeats, which is at or above the expansion threshold, and is dependent on the locus and disease process. For Huntington's disease the disease-causing threshold is 38–40 repeats, and is governed by the length at which the polyglutamine

tract (coded for by CAG) within the Huntingtin gene becomes toxic. At the myotonic dystrophy locus, the disease threshold is closer to 200 repeats, the size at which the CUG RNA exerts toxic effects on muscle cells [2,4].

It is well established that in mammalian cells, proteins with an abnormally long polyglutamine tract due to a CAG expansion cause toxic effects that ultimately result in cell death [2-3]. In addition, RNA containing a long CUG tract can also cause toxicity and cell death by sequestering RNA binding proteins, as happens in patients with myotonic dystrophy where the expanded CTG repeat is transcribed but not translated [2-3]. However, less is known about whether the expanded repeat DNA itself is toxic to cells.

CAG repeats of 55–80 repeats have been shown to block replication fork progression in plasmids, cause fork reversal on a eukaryotic chromosome [5-7], and interfere with ligation of 5' DNA flaps that occur during Okazaki fragment maturation or gap repair [8-9]. Structure-forming trinucleotide repeats also cause double-strand breaks (DSBs) in a length-dependent manner resulting in chromosome fragility [10-11]. Thus multiple types of DNA damage occur at an expanded trinucleotide repeat tract, including stalled or reversed forks, single-strand breaks or gaps, and double-strand breaks (DSBs). Our recent results have shown

## Author Summary

Expansion of a CAG/CTG trinucleotide repeat is the causative mutation for multiple neurodegenerative diseases, including Huntington's disease, myotonic dystrophy, and multiple types of spinocerebellar ataxias. Two reasons for the cell death that occurs in these diseases are toxicity of the repeat-containing RNA and of the polyglutamine-containing protein product. Although the expanded repeat can interfere with DNA replication and repair, it was not known whether the presence of the repeat within the DNA causes any additional cellular toxicity. In this study, we show that an expanded CAG/CTG tract placed within the chromosome of the model eukaryote, budding yeast, elicits a cellular response that interferes with cell growth and division. The effect is enhanced when DNA repair pathways, particularly double-strand break repair, are compromised. Moreover, cells experiencing an arrest were more likely to have undergone further repeat expansions. We show that the conserved MRX protein complex locates to the expanded repeat and is required to sense the damage and activate the DNA damage response. Our results suggest that DNA damage at expanded CAG/CTG repeats could contribute to both tissue degeneration and further repeat instability in affected individuals.

that DSBs at expanded CAG tracts are healed by both Rad52-dependent homologous recombination (HR) and Dnl4 (Lig4) mediated end joining (EJ) pathways, and that integrity of the MRX complex (Mre11/Rad50/Xrs2) is critical for preventing chromosome fragility at CAG repeats [12]. Given the evidence that these structure-forming repetitive DNA elements are damage-prone, it is critical to determine whether they are capable of eliciting cell cycle checkpoint responses independent of defects in RNA or protein metabolism.

Sites of DNA damage recruit proteins directly involved in DNA repair or fork restart as well as checkpoint proteins [13-14], and the persistence of DSBs or stalled forks in mutants deficient for key checkpoint factors suggests that repair mechanisms are aided by cell cycle checkpoint activation [15-16]. Recruitment and activation of a checkpoint protein triggers a signaling cascade mediated by substrate phosphorylation, leading to downstream responses such as halting cell cycle progression to allow time for repair. The Rad53 (Chk2) checkpoint kinase is the central effector of the DNA damage checkpoint in *S. cerevisiae* [16-17]. Activation of Rad53 in S phase leads to inhibition of late origin firing, stabilization of stalled replisomes, and a slowing of S phase progression in what is referred to as the S phase checkpoint, although there is no actual S phase arrest and cells will eventually enter G2 [18-19]. Not all checkpoint activation leads to a noticeable cell cycle delay, especially when the damage is repaired quickly [20]. However if the damage is not repaired in a timely manner, an extended checkpoint arrest will ensue, and cells will accumulate at the G2/M boundary. In yeast, a cell harboring a single, irreparable DSB can adapt to the damage after 8–10 hours and continue cycling; the damage may be then be repaired in a subsequent cycle [21-23]. In both yeast and mammalian cells, persistence of the damage will eventually result in cell death [24-25]. Thus induction of a DNA damage checkpoint can either facilitate repair or lead to cell death, depending on the severity of the damage.

The DNA damage checkpoint has been primarily studied as a response to exogenous damage to the genome by agents that cause fork stalling, base damage, or DSBs. However less is known about the response to endogenous sequences with the potential to form

non-B DNA structures. Previous genetic evidence in *S. cerevisiae* indicated that checkpoint proteins were involved in CAG repeat tract maintenance, suggesting that expanded repeats accumulate damage that is sensed by the cell cycle checkpoint machineries. Mutation of genes central to the DNA replication and DNA damage checkpoints including *MEC1*, *MRC1*, *RAD24*, *RAD17*, and *RAD53* resulted in elevated rates of repeat-mediated chromosome fragility and instability [26-28]. Particularly, deletion of genes that sense and transduce the replication checkpoint response, *MRC1*, *MEC1*, and *RAD53*, led to the greatest increase in CAG fragility [26-27]. Although these checkpoint proteins are crucial for preventing or healing CAG breaks, direct evidence for whether the expanded repeats activate cell cycle arrests, if so at what frequency, and any consequence for cell growth and viability, was lacking. Using cell cycle, biochemical and functional assays that can measure the robustness of checkpoint activation in repeat-containing cells, we report the novel observation that damage at structure-forming (CAG)<sub>70</sub> or (CAG)<sub>155</sub> repeats has the potential to activate DNA damage checkpoints, interfere with normal cell cycle progression, and compromise cell proliferation and survival in *S. cerevisiae*.

## Results

### Microcolony assay to determine if a population of CAG repeat-containing cells has a growth disadvantage

Our earlier results indicated that checkpoint proteins are required in cells containing expanded CAG repeats in order to prevent increased fragility and instability of the repeats [26-27]. However, as these results were partly obtained using genetic assays that could detect rare events, it was not known if checkpoint activation in repeat-containing cells is a rare or common event, or whether it results in cell cycle delays. Therefore we sought to determine whether an expanded CAG repeat causes measurable effects on cell growth. We used a yeast strain containing a yeast artificial chromosome (YAC) with either no repeat (CAG-0) or an expanded CAG repeat originally cloned from a myotonic dystrophy patient [29]. The repeat was cloned into a region of the YAC not predicted to be transcribed or translated, and flanked by minimal human sequence, 50 bp and 150 bp on each side the repeat. In general, two allele sizes were studied, 70 and 155 repeats, which have been previously shown to exhibit both instability and fragility at this location [29]. Preliminary experiments in liquid culture revealed slight delays in exponential growth of wild-type yeast containing a CAG-195 repeat at this location (Figure S1). However, because bacterial cells with contracted repeats have a growth advantage in liquid culture over those with longer repeats [30], and since about 30% of CAG-155 repeats have a contraction event in wild-type (WT) yeast [29], we reasoned that the observed repeat-induced growth inhibition could be an underestimation. Therefore, a microcolony experiment, which measures population viability of cells on solid media, was performed to assess the extent of repeat-mediated growth inhibition. This experiment is similar in principle to that performed by Weinert and Hartwell [31], which originally described mutants that escaped the control of DNA damage checkpoints in *S. cerevisiae*.

Unbudded G1 cells were micromanipulated onto YC-Leu solid media that maintained selection for the repeat-containing chromosome, and their growth into microcolonies (small colonies, visible under the microscope) was monitored (Figure 1A). Since no essential genes required for cell survival are located in close proximity to the repeat, the growth differences observed between cells with or without the CAG tract can be attributed to a repeat-

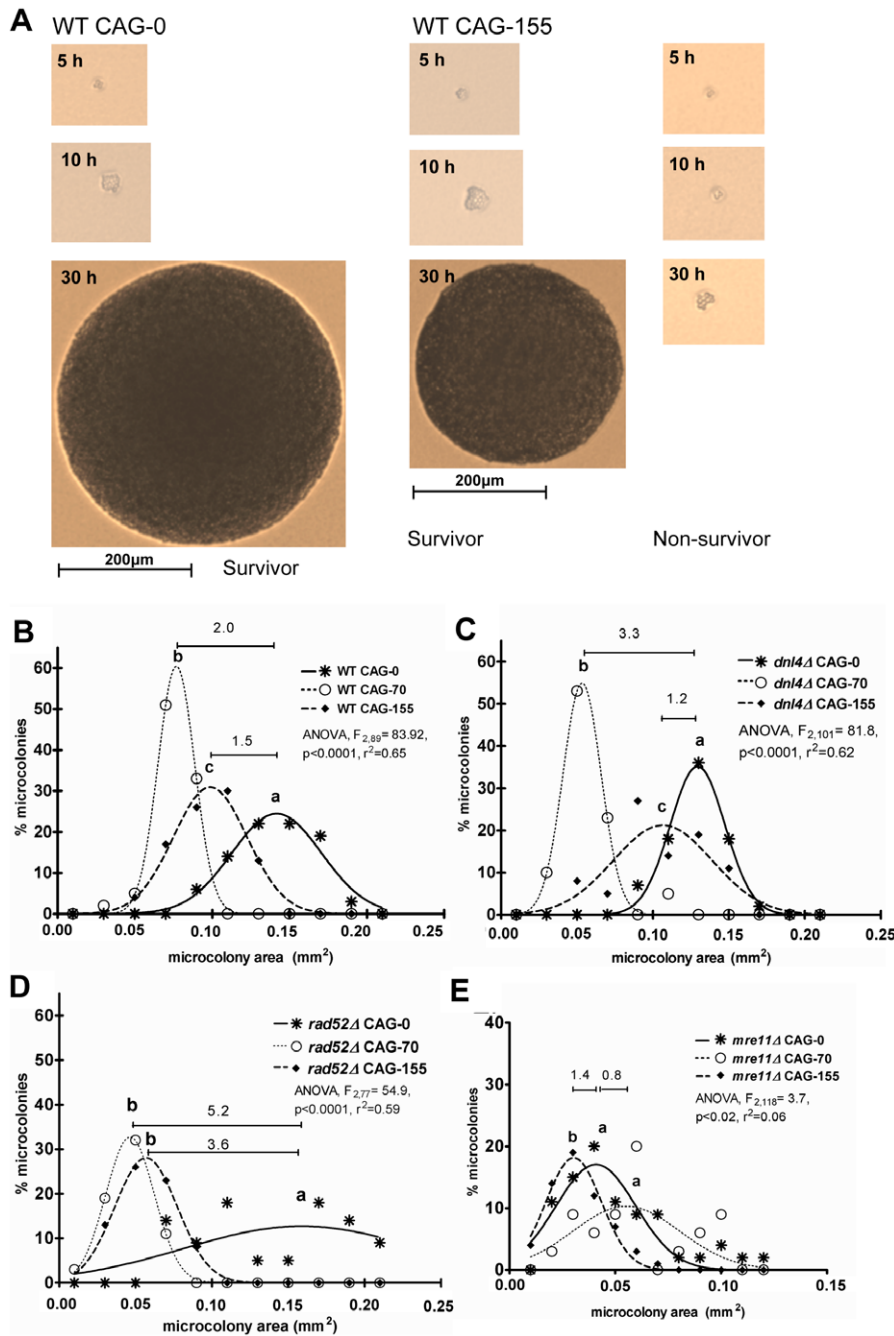


**Figure 1. Microcolony assay to detect cell growth defects.** (A) Examples of colony growth at 5, 10, and 30 hours in wild-type (WT) cells without or with a CAG-155 repeat tract. (B–E) Frequency size distribution of *dnf4Δ* (B), *rad52Δ* (C) and *mre11Δ* (E) survivors at 30 hours (area of  $\geq 0.01$  mm<sup>2</sup> at 30 hours). Numbers above bars between survivor peaks represent mean distance ratios, quantifying the severity of growth inhibition of the repeat-containing strain compared to the CAG-0 control strain. Letters ‘a’, ‘b’, or ‘c’ above peaks indicate statistical differences among CAG-0, CAG-70 and CAG-155 strains within a genotype; statistical similarities are denoted by the same letter. Non-survivors that failed to divide past  $\sim 6$  divisions ( $\leq 0.005$  mm<sup>2</sup>) are not shown.  
doi:10.1371/journal.pgen.1001339.g001

mediated effect. A typical *S. cerevisiae* cell cycle time of 2 hours on synthetic media would result in about 15 doublings at 30 hours of growth. At 30 hours, we observed a bimodal distribution of microcolony growth in WT CAG-70 or CAG-155 strains. This distribution typically consisted of “survivors” (area  $\geq 0.01$  mm<sup>2</sup>, more than 6 doublings, Figure 1A–1E) and “non-survivors” (area  $\leq 0.005$  mm<sup>2</sup>, 6 or fewer doublings). The non-survivors likely represent terminally arrested lineages (frequencies, reported

in [12], were  $\sim 10\%$  for WT cells with or without a CAG repeat). Among survivors, WT CAG-70 or CAG-155 strains showed a significant 1.5 to 2-fold decrease in mean microcolony area compared to the WT CAG-0 control strain (Figure 1B). Therefore, in the WT strain, a large enough proportion of the cells containing an expanded CAG repeat experienced a growth delay that the overall rate of population growth was affected. We have seen the same effect in two other yeast strain backgrounds,

(A. LaPorte, C. Weindel, and C.H. Freudenreich, data not shown).

We also assessed the survival efficiency of mutants lacking end-joining (*dnl4Δ*), homologous recombination (*rad52Δ*) or the MRX complex (*mre11Δ*) because we showed that all three of these pathways act to repair breaks at expanded CAG-70 or -155 repeats [12]. The *dnl4Δ* strain exhibited a pattern similar to WT, with CAG-70 and CAG-155 microcolonies attaining a mean area 3.3-fold and 1.2-fold below the CAG-0 control respectively (Figure 1C). The *rad52Δ* CAG-70 and CAG-155 microcolonies attained mean sizes 5.2 and 3.6-fold below CAG-0, revealing that the presence of expanded repeats significantly inhibited population growth in this background and more severely than in the WT strain (Figure 1D). Overall, the extent of repeat-induced growth inhibition depended on both the length of the repeat and the nature of the repair defect: Rad52 deficiency severely impacted the viability of both CAG-70 and CAG-155 survivors, while the Dnl4-EJ pathway deficiency impacted the viability of cells with 70 repeats more than those with 155 repeats, a trend that was present in all three backgrounds but was more pronounced in the *dnl4Δ* mutant.

Surprisingly, the repeat-induced growth defect phenotype observed in the *rad52Δ* and *dnl4Δ* repair mutants was absent among *mre11Δ* survivors (Figure 1E). Deletion of *MRE11* caused a significant growth defect in all cells, with or without an expanded CAG repeat. The broader area distribution and relatively smaller colony sizes of both *rad52Δ* CAG-0 and *mre11Δ* CAG-0 strains indicate that a wide spectrum of sporadically occurring damage in addition to CAG repeat damage require HR and MRX pathways for viability. However, the slow growth phenotype of the *mre11Δ* CAG-70 strain, rather than being enhanced, was somewhat relieved relative to CAG-0 or CAG-155 strains. This striking phenotype suggests that a proportion of damage that occurs at a CAG-70 repeat can escape detection by the cell cycle checkpoint machinery in the absence of the MRX complex. In addition to the effects graphed in Figure 1, a significant 3.5-fold increase in the frequency of non-survivors was observed in strains with CAG-70 or -155 repeats compared to the CAG-0 control in the *rad52Δ* and *mre11Δ* backgrounds, an effect not observed in wild-type or *dnl4Δ* strains [12]. Collectively, the above phenotypes indicate that repeat-containing cells have a proliferation defect frequent enough to result in reduced population viability, and that deficiency of DSB repair pathways exacerbates the defect.

### Single cell pedigree analysis reveals repeat-induced growth arrests with aberrant cell morphology

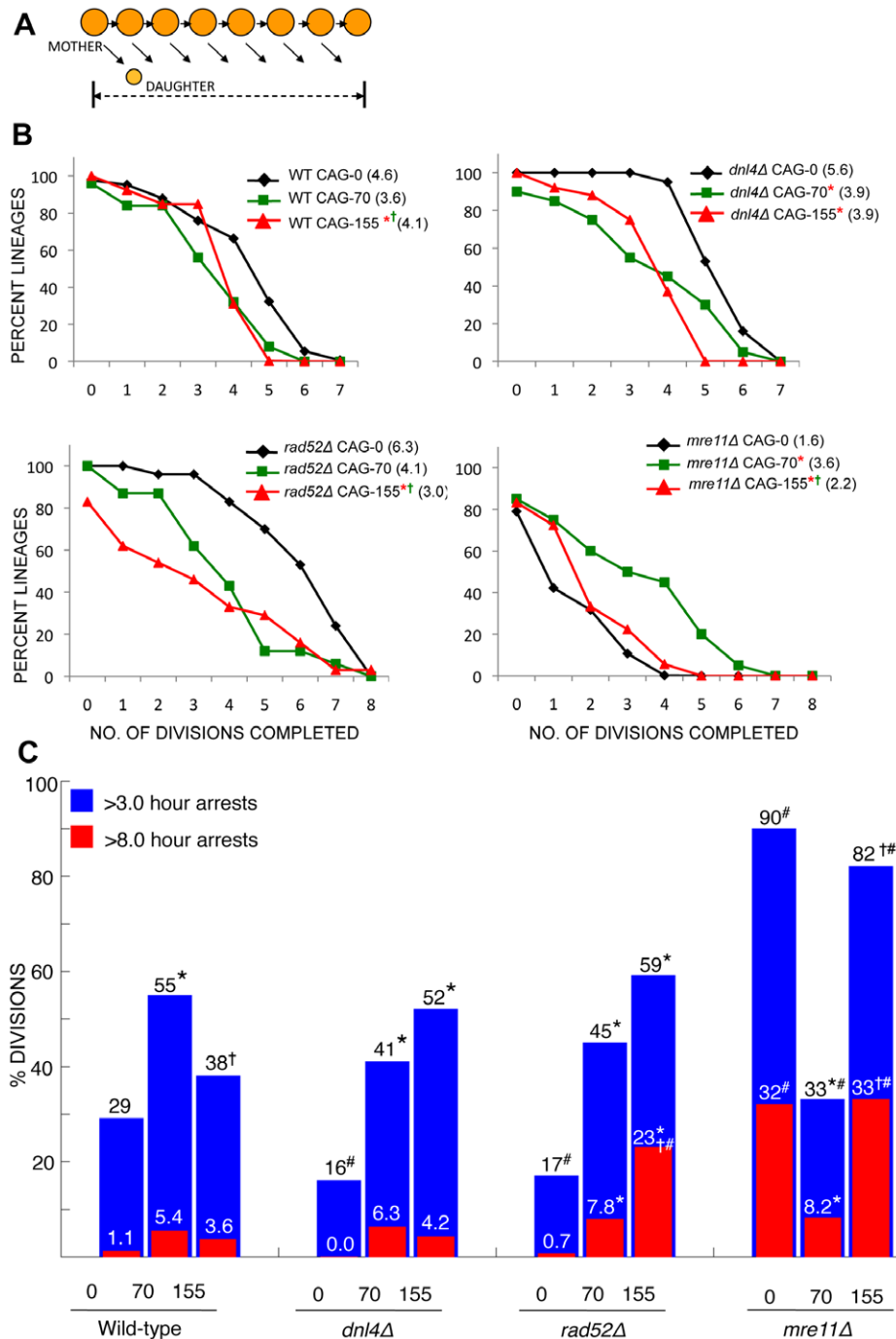
To better understand the basis of smaller microcolony sizes and reduced population viability of repeat-containing cells, a single cell pedigree analysis was performed. Single precursor cells were micromanipulated onto YC-Leu solid media, and successive divisions were followed for a span of ~18 hours, micromanipulating the daughter cells away at each division in order to follow a single lineage (Figure 2A). For each strain, about 30 lineages were analyzed for 5–7 divisions per lineage, for an average of 90 cell divisions per strain (Table S1). We first analyzed the division potential of each lineage, i.e. the ability of a progenitor cell with an expanded CAG repeat to sustain successive divisions in a lineage (Figure 2B). In the wild-type background, the CAG-70 and CAG-155 repeat-containing strains completed on average fewer divisions per lineage (3.6 and 4.1) than the CAG-0 no-tract control strain (4.6). This difference was even more striking in *dnl4Δ* and *rad52Δ* backgrounds, with fewer divisions completed compared to the no repeat control and some lineages failing to complete even one division (e.g. 60% for *rad52Δ* CAG-155,

Figure 2B). Similar to the microcolony analysis, the profile was altered in the *mre11Δ* strain, with CAG-70 cells exhibiting a greater division potential than either CAG-0 or CAG-155 strains. This result supports the conclusion that damage at the CAG-70 tract is not being properly sensed or signaled in the absence of the MRX complex. This conclusion is further substantiated by a decreased frequency of cell-cycle arrests and decreased morphological defects in *mre11Δ* CAG-70 cells compared to *mre11Δ* CAG-0 and CAG-155 cells (see below, Figure 2C and Figure 3B).

To determine if reduced division potential was due to frequent cell cycle arrests, divisions were either categorized as normal divisions, lasting <3.0 hours, or arrest divisions, lasting >3.0 hours. While a majority of divisions in the WT CAG-70 and CAG-155 strains were normal divisions (cycling time of <3 hours), 55% and 38% of divisions, respectively, were >3 hour arrest divisions, an elevated frequency compared to the WT CAG-0 control (29%; Figure 2C). Both *dnl4Δ* and *rad52Δ* strains showed a further disparity between repeat-containing and no-tract control strains, with a 2.6-fold increase for CAG-70 and 3.3 to 3.5-fold increases for CAG-155 strains in the frequency of >3 hour divisions (Figure 2C). For the *rad52Δ* CAG-155 strain, about 60% of divisions took longer than 3 hours, compared to only 17% in the *rad52Δ* CAG-0 control. Thus the presence of an expanded CAG repeat had the potential to prolong cell division in a large proportion of cells, and arrests were 2 to 3-fold more frequent than in cells without an expanded repeat tract. The increased frequency of arrests explains the repeat-specific decrease in microcolony size and reduced division potential.

In addition to “normal” arrest times of 4–6 hours, we noted that a subset of arrests were very prolonged, >8 hours and up to 16 or more hours (the length of the experiment) (Figure 2C and Figure S2). Certain repair foci are known to last >8 hours in arrested cells, although yeast cells can also sometimes adapt after ~8 hours of arrest and re-enter the cell cycle even though the damage has not been repaired [21,32–33]. Adaptation coincides with release from arrest, re-entry into the cell cycle, and disappearance of Rad53 phosphorylated species [34]. WT CAG-70 and CAG-155 strains experienced >8 hour arrest divisions at a frequency 3 to 5-fold higher than the WT CAG-0 control (Figure 1C). Among the DSB repair-deficient mutants, 6.3% or 4.4% of *dnl4Δ* CAG-70 and CAG-155 strains experienced arrest divisions >8 hours, respectively, relative to 0% in the *dnl4Δ* CAG-0 control. The *rad52Δ* CAG-70 and CAG-155 strains experienced >8 hour arrests in 7.8% and 23% of divisions respectively, an 11- or 33-fold increase over the *rad52Δ* CAG-0 control. The higher frequency of >8 hour arrest divisions observed in repeat-containing cells suggests that expanded repeats are accumulating damage that is difficult to repair. Finally, among all comparisons, the dramatic increase in the frequency of >8 hour arrest divisions in the *rad52Δ* CAG-155 strain, which is 6.4-fold greater than the WT CAG-155 strain, indicates a requirement for Rad52-mediated HR in repairing damage at the CAG-155 repeat and ensuring timely cell cycle progression.

We further analyzed whether the arrests resulted in recovery, where the cell cycle resumed before 8 hours of arrest (usually indicating successful repair), adaptation, where the cell was arrested more than 8 hours but did eventually re-enter the cell cycle, or terminal arrests, which were not observed to re-enter the cell cycle. For wild-type cells, most arrest events were able to recover or adapt (96–100%), although the recovery frequency was lower for repeat-containing cells (Table 1). Cells lacking one of the main DSB repair proteins and containing a repeat tract were less likely to recover, and more likely to have an adaptation response or experience a terminal arrest. Notably, with the exception of the



**Figure 2. Single cell pedigree analysis of CAG/CTG repeat-containing cells.** (A) Pedigree analysis scheme: a yeast mother cell was micromanipulated onto solid media, and daughter cells separated and moved away upon each cell division, so that the duration and characteristics of each cell division could be monitored. The mother cell lineage was followed so that daughter cell growth delays were not a factor. The dotted arrow represents one lineage of 7 divisions. (B) Doubling efficiency curves were generated from an average of 30 lineages (range 15–41) per strain, each followed for ~18 hours. Strain name followed by mean number of doublings indicated in brackets. Comparisons are done on the distributions within a genotype, either between the CAG-0 control and CAG-70 or CAG-155 strains (\*), or between CAG-70 and CAG-155 strains (†); Symbols denote  $p < 0.05$  using a Wilcoxon's sum-rank test. (C) Graphical representation of frequency of arrest divisions (computed out of total # of divisions) that have lasted >3.0 hours (in blue) or >8.0 hours (in red); the >8 hr values are a subset of the >3 hr values, and therefore overlaid on the >3 hr bars (not stacked). Statistically significant comparisons to CAG-0 (\* $p < 0.05$ ) or between CAG-70 and CAG-155 strains († $p < 0.05$ ) within genotype are indicated; statistics performed by logistic regression analysis. Comparison to WT of the same tract length (#,  $p < 0.01$ ) by Fisher's exact test. doi:10.1371/journal.pgen.1001339.g002

*mre11*Δ mutant, terminal arrests were not observed in the CAG-0 control strain even in *rad52*Δ or *dnl4*Δ backgrounds, suggesting that the presence of an expanded repeat can lead to a more severe

outcome than deficiency in a major DSB repair pathway. However the most striking difference between cells with and without an expanded repeat was the likelihood of experiencing a



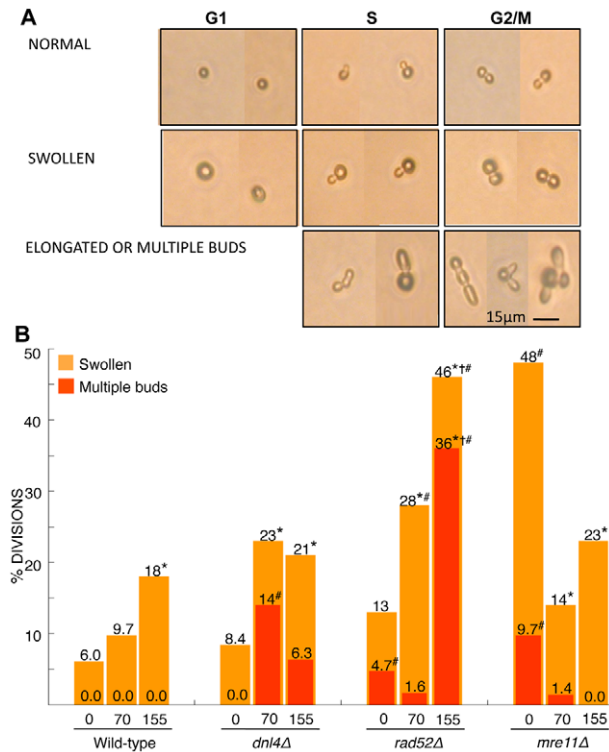


**Figure 3. Analysis of cell swelling and morphological defects in CAG/CTG repeat-containing cells.** (A) Representative micrographs of *S. cerevisiae* cells with expanded CAG-70 or -155 repeats experiencing an aberrant cell division cycle (G1, S or G2/M arrests) with either a swelling response or an abnormal morphology such as elongated or multiple buds. Cells undergoing a normal cell division cycle with normal morphology are included for comparison. The multibudded phenotype did not necessarily represent terminal arrests because cells were occasionally able to complete divisions despite this deformity. The size of swollen cells as quantified by NIH ImageJ software, was up to 5X the size of a normal cell; size correlated with length of the repeat and arrest duration. (B) Percent of divisions associated with swelling (light orange bars) or with both swelling and morphological defects (overlaid dark orange bars). Symbols as in Figure 2C. doi:10.1371/journal.pgen.1001339.g003

second arrest in the next cell division, as these recurring arrests appeared only in repeat-containing lineages (Table 1). This phenomena was repeat-length dependent, occurring more often in cells with a CAG-155 than CAG-70 repeat, and the second arrest was often longer than the first. Apparently, the damage at a repeat tract can sometimes persist through mitosis, causing a second arrest in the next cell cycle.

It is known that yeast cells undergoing a protracted arrest will often exhibit abnormal morphology, including swelling and elongated or multiple buds [35-36]. Indeed, we noted these phenotypes were increased in repeat-containing cells compared to the no repeat control (Figure 3). Several of the trends noted in our other assays were confirmed by comparing the occurrence of abnormal morphology: the occurrence of a swollen or multi-budded phenotype was exacerbated by increasing repeat length, with the Rad52 protein appearing to be particularly important for preventing CAG-155 repeat-induced effects, and the Dnl4 protein being either equally required at the two repeat lengths or slightly more so at CAG-70. In contrast, for the *mre11Δ* mutant, the repeat-containing cells had less severe swelling than the no-tract control and multi-budded cells were minimal to absent. This profile indicated that the repeat-induced checkpoint was bypassed

in this background, especially in the CAG-70 strain, unlike other non-repeat damage that was sensed and induced a response (Figure 3B). Cytokinesis defects and cell swelling similar to those observed in the repeat-containing cells have been documented in cells exposed to hydroxyurea (HU), which depletes nucleotide pools and results in slowing or stalling of replication forks [36-37]. We confirmed that a WT CAG-0 strain treated with a sub-lethal dose of HU exhibited a 2 to 3-fold increase in swollen and multi-budded cells (Figure S3). These data implicate replication stress as one likely cause of the phenotypes observed in the repeat-containing cells.

In summary, our results indicate that expanded CAG repeats have the potential to induce a protracted cell division cycle accompanied by frequent swelling and morphological defects, all of which are phenotypes that occur during activation of DNA damage checkpoints. These phenotypes were exacerbated in backgrounds deficient for either end joining or homologous recombination repair, and in contrast were mitigated by the absence of the Mre11 protein, especially for a CAG-70 repeat tract.

### Damage at expanded CAG/CTG repeats elicits frequent S phase and post-replication G2/M delays

In order to determine at what point in the cell cycle delays were occurring, and thereby gain insight into the potential types of damage causing the delays, we determined the cell cycle distribution of growth arrests. The frequencies of G1, S and G2/M arrests were recorded in wild-type or mutant cells with or without an expanded repeat tract (Figure 4A). Analysis of individual divisions from the pedigree experiment revealed that wild-type repeat-containing cells showed a bias towards arresting in the S and G2/M cell cycle phases relative to a CAG-0 control (Figure 4A). Specifically, the CAG-70 strain exhibited a modest but significant increase in S phase arrests (to 33% vs. 28% for CAG-0) and a greater tendency to arrest in G2 (51% vs. 40%), whereas the CAG-155 strain exhibited a further increase in frequency of arrests that began in S phase (38%). The profile was shifted dramatically in a *rad52Δ* strain, with the vast majority of the arrests occurring in the G2 phase (71-93%; absolute percentages are 2.8 and 2.7-fold over CAG-0, Table S1). Furthermore, the increase in S phase arrests in cells with a CAG-155 repeat was evident in the *rad52Δ* background and was highly significant compared to *rad52Δ* CAG-0 or CAG-70 (26% vs. 7-8%, Figure 4A). Altogether, these data suggest that the CAG-155 repeat results in a perturbation of replication that is severe enough to cause a slowing of S phase, while the damage at CAG-70, although it may also originate in S phase, does not always induce the S phase checkpoint but rather is more often resolved in G2. Furthermore, Rad52-dependent HR is apparently a crucial pathway for repairing repeat-induced DNA damage, a result consistent with the increased repeat tract fragility observed in a *rad52Δ* strain [12]. Shifts in arrest phase also occurred in repeat-containing *dnl4Δ* and *mre11Δ* cells; the majority of arrests in the absence of either protein were at the G2/M boundary, with *mre11Δ* cells additionally exhibiting a reduction in G1 arrest frequencies compared to the CAG-0 control (Figure S4).

To determine whether repeat-specific S and G2 arrests were also visible at a population level, cell cycle distributions were analyzed by flow cytometry (FACS). In this method, all cells are analyzed, not just those undergoing an arrest. The S phase slowdown was more difficult to detect by FACS than single cell analysis, but the tendency of WT repeat-containing cells to accumulate with 2N DNA content (G2/M) was evident (Figure 4B). In contrast, the WT CAG-0 strain contained mostly

**Table 1.** Modes of exit from cell cycle arrest.

Strain Background	% Recovery response >3<8 hours	% Adaptation response >8<14 hours	% Terminal arrests >14 hours	% Recurring arrests >3 hours
WT CAG-0	96	3.8	0	0
WT CAG-70	90 *	5.8	3.9	11 *
WT CAG-155	90	10	0	13 *
<i>dnl4Δ</i> CAG-0	100	0	0	0
<i>dnl4Δ</i> CAG-70	84 *	9.4	6.3	0
<i>dnl4Δ</i> CAG-155	92 *	6.0	2.0	17 *
<i>rad52Δ</i> CAG-0	96	4	0	0
<i>rad52Δ</i> CAG-70	83 *	14 *	3.4	13 *
<i>rad52Δ</i> CAG-155	62 *	31 *	7.7	36 *
<i>mre11Δ</i> CAG-0	64	25	11	0
<i>mre11Δ</i> CAG-70	77 *	15 *	7.7	29 *
<i>mre11Δ</i> CAG-155	62	29	8.8	31 *

Percentages are out of total number of >3 hr arrests. \*  $p < 0.05$ . Statistical significance was determined by logistic regression analysis (columns 1–3) or Fisher's exact test (column 4).

doi:10.1371/journal.pgen.1001339.t001

cells with 1N DNA content (G1/G0) near stationary phase. In the *rad52Δ* background, the proportion of cells that accumulated with 2N DNA content was increased even in the CAG-0 control but was further increased in the CAG-155 strain, confirming the importance of this protein for repair of repeat-induced damage in addition to spontaneous damage occurring within non-repetitive regions.

Based on the above phenotypes, we conclude that expanded CAG repeats have the potential to induce both the intra-S and G2/M DNA damage checkpoints. Our results show that specific S and G2/M phase arrests, as opposed to a general overall slowed progression through the cell cycle, contribute to longer cell division times in repeat-containing cells. Rad52-dependent homologous recombination is particularly crucial for prevention of S phase delays and release from the G2/M block to allow resumption of cell proliferation.

### CAG expansion events are frequently associated with cell cycle delays

Since the above results indicated that checkpoint-mediated cell cycle arrests are associated with a repair or fork restart event, we wished to determine the status of the CAG repeat locus in cells that had experienced an arrest. Due to technical difficulty in amplifying the repeat from a single arrested cell, two approaches were taken. First, we isolated swollen cells (one indicator of arrest, Figure 3B), allowed them to divide to form colonies, and then assessed repeat length in the resulting colonies. To obtain a large enough sample size the analysis was done in the *rad52Δ* CAG-70 background. 70% of these swollen cells did not form a colony, being permanently arrested or dead. Among the remaining 30% that formed normal-size colonies, there were 14% contractions and 4.8% expansions (Table 2), frequencies that are almost identical to CAG-70 tract instability in *rad52Δ* colonies not selected for originating from swollen precursor cells (15% and 5.9%, [12]). In the second approach, cells were not preselected, but repeat length was determined only for colonies that grew poorly, which were presumably enriched for cells experiencing arrests. Strikingly, the poorly growing colonies had a large increase in the frequency of total instability, to 67%, compared to 21% for *rad52Δ* CAG-70 normally growing colonies (Table 2). The

increase in instability was biased toward expansions, with a 2-fold increase in contractions and a significant 6-fold increase in expansions (Table 2). These results indicate that the cell cycle delays observed in CAG repeat-containing cells are frequently associated with mis-repair events resulting in repeat instability.

To determine whether impaired replication fork movement could contribute to repeat instability, we determined CAG-70 tract stability in wild-type cells exposed to a sub-lethal dose of hydroxyurea (0.1 M). Treatment with hydroxyurea resulted in a 7-fold increase in expansions (to 5.6%), relative to the untreated control (0.8%,  $p < 0.01$ , Table 2). Contractions remained similar to the untreated wild-type control. We conclude that these HU-dependent expansions, which occurred independently of Rad52-HR (data not shown), result from impaired replication across the repeats. These data suggest that the expansions that arose in the *rad52Δ* poorly growing colonies could be due to slippage events at slowed or restarting replication forks. We showed previously that Rad52- and Dnl4-dependent DSB mis-repair events are other mechanisms for generation of expansions [7,12].

### An expanded CAG tract induces Rad53 phosphorylation and Mre11p localization

The above results show that cell cycle checkpoints are activated in response to damage or interference with fork progression at an expanded CAG repeat. If the level of repeat-induced damage is sufficient or present in a large-enough proportion of cells, phosphorylation of the Rad53 checkpoint kinase should occur. Therefore, we directly tested the phosphorylation status of Rad53 in CAG repeat-containing cells.

The wild-type strain harboring a CAG-155 repeat failed to show a detectable shift in mobility of the Rad53 protein, similar to the CAG-0 control (compare lanes 2 and 3, Figure 5A). Because CAG fragility is proportional to increasing repeat length [29,38], CAG-195 and CAG-240 repeat lengths were also tested, however a phosphorylated Rad53 species was still not detectable (Figure 5A). In contrast, control samples treated with 0.05% MMS or 0.1 M HU exhibited Rad53 phosphorylation, although the intensity and size of the shifted species was considerably less with HU relative to MMS treatment. Since the wild-type strain has functional repair pathways, the lack of detectable Rad53

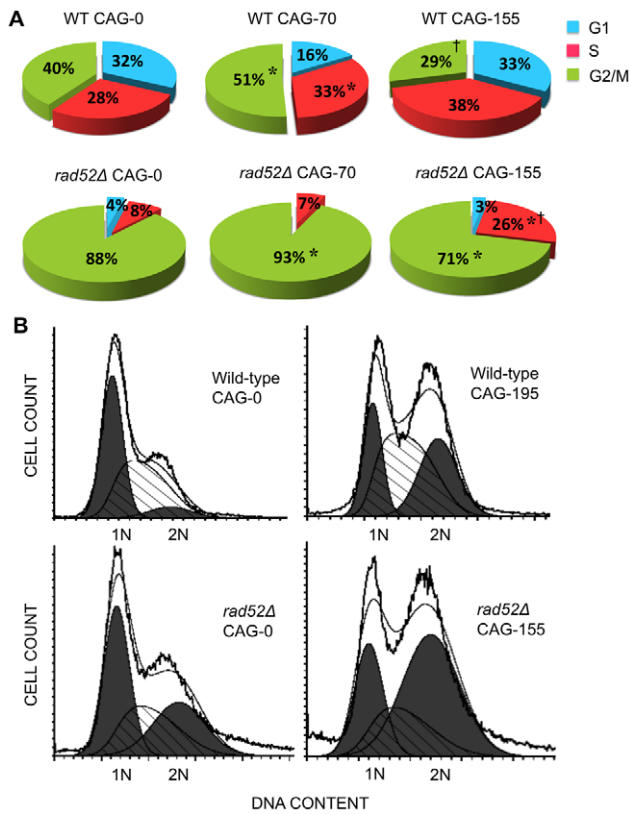


**Figure 4. Cell cycle position of arrests.** (A) Indicates cell cycle position of arrests (>3.0 hrs) observed for actively dividing cells on YC-Leu solid media in the single cell pedigree analysis. Arrests defined as >60' for G1, >45' for S, >60' for G2/M. Not included are normal divisions <3.0 hours that showed an S phase or G2/M delay. Statistically significant comparisons to CAG-0 (\*) or between CAG-70 and CAG-155 strains (†) within genotype are indicated. Statistics performed by logistic regression analysis on raw data calculated out of total # of divisions (Table S1). (B) FACS analysis of DNA collected from wild-type or *rad52Δ* cells in near-stationary phase liquid cultures, with 0, 195, or 155 repeats. Unfilled curves show DNA content, either raw data (jagged line), or smoothed data generated by ModFit software. Filled and hatched histograms denote putative G1 or G2 and S phases, respectively.  
doi:10.1371/journal.pgen.1001339.g004

phosphorylation could be due to either successful repair of CAG-associated damage or a level of phosphorylated species too low to be visible as a mobility shift on the gel. Indeed, only 3.6% of WT

CAG-155 cells exhibited arrests >8 hrs (Figure 2C). Therefore, we monitored the Rad53 phosphorylation status in *rad52Δ* cells that showed a greater frequency of long arrests (7.8% and 23% for CAG-70 and -155 respectively), and elevated CAG fragility [12]. Indeed, *rad52Δ* CAG-70 or CAG-155 strains but not the *rad52Δ* CAG-0 control showed a discernible Rad53 phosphorylation response (Figure 5B), indicating that the DNA damage checkpoint is activated in a repeat-dependent manner in this mutant background. The level of Rad53 phosphorylation was repeat-length dependent with the longer CAG-155 repeat eliciting a more robust checkpoint response than the intermediate CAG-70 repeat length as determined by densitometric quantification (Figure 5B, right). We conclude that in the absence of Rad52-dependent repair, the types of damage that occur at an expanded CAG repeat induce a signaling cascade that results in Rad53 phosphorylation and associated downstream checkpoint events. Based on the data from the microcolony and pedigree experiments, it is likely that the same events happen in a wild-type background, but the damage is at a lower level or repaired more quickly so that phosphorylated Rad53 does not accumulate to a level detectable by Western blotting.

To determine whether CAG repeat damage was capable of eliciting a cell cycle checkpoint response in the absence of the MRX complex, we determined the Rad53 phosphorylation status in *mre11Δ* cells. The results revealed two surprising observations. First, Rad53 phosphorylation was observed in *mre11Δ* CAG-70 and CAG-155 strains (Figure 5C), even though CAG-70 cells, and to a lesser degree CAG-155 cells, appeared to escape cell cycle arrests in this background (Figure 1, Figure 2, Figure 3). Second, Rad53 phosphorylation was also observed in *mre11Δ* CAG-0 cells, a pattern unlike the WT and *rad52Δ* CAG-0 controls. Based on these results, we infer that the local checkpoint signaling in response to CAG damage is compromised in *mre11Δ* cells, while global checkpoint signaling in response to non-repeat damage in the genome is intact. A local Mre11-dependent response at the repeat is further supported by physical detection of the Mre11 protein at the repeat tract, which is enhanced 12-fold compared to a non repeat reference locus by chromatin immunoprecipitation (ChIP) (Figure 5C, right). Intriguingly, Mre11 localization to the repeat peaks in S phase, suggesting that the relevant structure sensed by Mre11 is formed during DNA replication.

In conclusion, an expanded CAG repeat at a single genomic locus can induce a myriad of cellular arrest responses that depend on signaling via the MRX complex, and culminating in a detectable Rad53 phosphorylation response if the damage is not promptly or efficiently repaired by Rad52-dependent recombination.

**Table 2. CAG-70 repeat instability in colonies exhibiting poor growth due to frequent arrests or treated with 0.1 M hydroxyurea.**

Genotype / Treatment	Precursor cell and colony morphology	# colonies tested	% Instability	% Expansions	% Contractions
<i>rad52Δ</i> <sup>a</sup>	normal cell→normal colony	204	21	5.9	15
<i>rad52Δ</i> <sup>b</sup>	swollen cell→normal colony	21	19	4.8	14
<i>rad52Δ</i>	normal cell→poorly growing colony <sup>c</sup>	12	67 **	33**	33
WT (-HU) <sup>a</sup>	normal cell→normal colony	243	6.6	0.8	5.8
WT (+HU)	normal cell→normal colony	195	10	5.6**	4.6

**a** data from Sundararajan et al. (2010) [12] included for comparison, **b** swollen cells isolated by micromanipulation, **c** very small colonies after 3 days growth; repeat expansions were +10 to +20 repeats. Statistical significance determined by Fisher's exact test, \* p<0.05, \*\*p<0.01, upon comparison of with normal untreated colonies of same genotype.

doi:10.1371/journal.pgen.1001339.t002



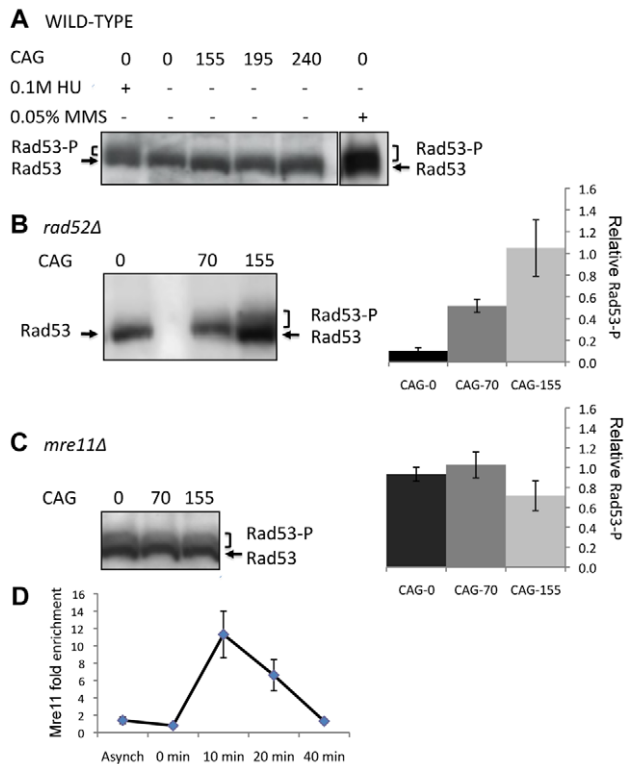


**Figure 5. Rad53 phosphorylation status and Mre11 localization in strains with expanded CAG/CTG repeats.** Western blots of protein extract from (A) WT (B) *rad52Δ*, and (C) *mre11Δ* cells probed with Rad53 antibody. Extracts treated with 0.1 M HU (A, lane 1) or 0.05% MMS (A, lane 6) are included as positive controls. Quantified equal amounts (15 ng) of total protein prepared from asynchronous cultures were loaded per lane; the positions of unphosphorylated Rad53 (93 kDa) and hyperphosphorylated Rad53 species (Rad53-P) are indicated by arrows and square brackets, respectively. Rad53 hyperphosphorylated species were quantified and normalized to the Rad53 intact band; average of 3 experiments with standard error of the mean (SEM) is shown for *rad52Δ* (B, right) or *mre11Δ* (C, right) strains. Similar ratios were obtained when Rad53-P signal was normalized to an internal loading control (data not shown). (D) Mre11-TAP is recruited to the CAG repeat-containing DNA fragment. A strain with TAP-tagged Mre11 and a CAG-155 repeat was used for CHIP. Chromatin samples were collected from cultures either unsynchronized (Asynch) or synchronized in G1 with  $\alpha$ -factor, released into S phase, and samples collected at the indicated time points. Fold enrichment of Mre11 at the CAG repeat (y-axis) was obtained by normalizing PCR product amplification efficiency from DNA adjacent to the CAG repeat (CAG IP/WCE) to a control PCR product from the *ACT1* locus (*ACT1* IP/WCE). Error bars represent SEM. doi:10.1371/journal.pgen.1001339.g005

## Discussion

Despite the knowledge that expanded CAG repeats interfere with replication, nick ligation, and are fragile sites, direct evidence on whether such damage is at a level or type sufficient to activate DNA damage checkpoints was lacking. This question is especially important since repeated or long checkpoint arrests can affect cell growth potential and lead to apoptosis in higher eukaryotes. It is also of interest to better understand the cellular response to structure-forming sequences, since there are many examples of these sequences in the human genome. Using yeast containing an expanded CAG repeat, we were able to follow the growth potential and fate of single live cells. The presence of a CAG-70 or CAG-155 repeat did not elicit visible Rad53 phosphorylation by Western blot in wild-type cells. We were nonetheless able to detect

significant differences between cells with and without an expanded repeat in growth potential, number of arrests, duration of arrests, and morphological abnormalities. Thus even in a wild-type cell, the presence of a long repeat tract was a significant burden on the cell that resulted in measurable effects on growth and division potential. Notably, the arrests that occurred within repeat-containing cells were sometimes of a very long duration, greater than 8 hours and frequently accompanied by severe cell swelling, indicating that a type of damage had occurred that was particularly difficult to repair [21,32,34].

What is the origin of the damage inducing the checkpoint response? Recently, it was reported that convergent transcription through CAG repeats induces apoptosis in both dividing and non-dividing human cells [39]. Our CAG repeat is not within a gene or known transcriptional unit, however RT-PCR experiments did show low but equivalent levels of transcript in WT and *rad52Δ* cells, which could reflect read-through transcription from the neighboring *URA3* gene (M. Koch, J. Yang, and C.H. Freudenreich, data not shown). Therefore, it is possible that some of the damage may initiate during transcription. However, the similar transcript levels in the two strains, together with the S-phase delays, the S-phase binding by Mre11p, and the importance of Rad52-dependent repair are all more consistent with the primary damage sensed by the checkpoint occurring during DNA replication.

Whatever the initiating event, our data indicate that Rad52-dependent recombination is a key mechanism for overcoming repeat-dependent damage in cells, and without it a strong checkpoint response is induced and cellular growth is severely compromised. For the CAG-155 repeat-containing cells lacking Rad52, a quarter of the divisions displayed arrests of greater than 8 hours and 36% had morphological abnormalities. In addition, most of those cells had a recurring arrest in the next cell division, indicating that the damage had persisted. The checkpoint responses were all highly repeat-length dependent in the *rad52Δ* background being significantly greater at CAG-155 compared to CAG-70, indicating that damage at the longer repeat requires rescue by recombination mechanisms more frequently. In addition, the cell cycle analysis indicated that cells with a CAG-155 tract had a greater tendency to show an S phase delay compared to CAG-70, a difference exacerbated by Rad52 deficiency. We conclude from this data that the longer repeat has a greater effect on replication, and that a Rad52-dependent process is likely involved in fork restart events for this tract length. This interpretation is supported by comparatively increased CAG-155 fragility observed in a *rad52Δ* strain [12]. The CAG-70 repeat likely also interferes with replication, as there was a slight increase in S-phase delays, and we showed previously that Srs2-dependent fork reversal occurs at a CTG-55 repeat [7]. Perhaps at this repeat length, fork restart can usually occur without recombination, consistent with genetic results. However if fork reversal or integrity is compromised, recombination may become the preferred pathway, since the CAG-70 expansions that occur in *srs2Δ* or *mre11Δ* mutants are Rad52-dependent [7,12].

The Dnl4 ligase, needed to complete end-joining repair of DSBs, also played a role in preventing repeat-mediated cell cycle arrests and promoting normal growth and division potential. The requirement for end-joining was more subtle than that for HR, although deficiencies in either process led to a large percentage of cells arrested in G2 with 2N DNA content. While the Dnl4 protein strictly localizes to DSBs, the Mre11 and Rad52 proteins have also been found at stressed or collapsed replication forks and may aid in fork restart [40-41], potentially explaining the greater requirement for these proteins. Altogether, our data are consistent

with the idea that the expanded CAG repeat causes multiple types of damage sensed by the checkpoint, including stalled or reversed forks in S phase needing Rad52-dependent restart, and DSBs in G2 that can be repaired by either Rad52-dependent HR or Dnl4-mediated end joining. Importantly, cells which showed an initial arrest response but were able to continue dividing for a limited time to form small, poorly growing colonies showed a significantly elevated frequency of repeat instability. Thus repeat instability may preferentially occur during inefficient or initially failed repair or fork restart events.

Cell cycle arrest responses were dramatically altered in the absence of a functional MRX complex. In general, all *mre11Δ* cells, with or without a repeat tract, are quite compromised for growth with small microcolonies, a reduced division potential, a very high frequency of divisions arresting for >3 hrs (90% for CAG-0), and a third arresting for >8 hrs. Notably, although *mre11Δ* cells were often swollen due to the frequent and long arrests, they did not exhibit many morphological defects. Opposite to the situation in wild-type cells or other DSB repair mutants, the arrest and growth phenotypes were usually less severe in the *mre11Δ* repeat-containing cells, especially for the CAG-70 tract. Cells containing a CAG-70 tract and lacking the Mre11 protein had a relief of the microcolony growth defect, underwent significantly more divisions, fewer arrests and less cell swelling compared to CAG-0 cells. These results indicate that an intact MRX complex is required for efficient induction of the repeat-mediated checkpoint, and that the majority of CAG-70 damage and some of the CAG-155 damage likely escapes detection by the cell cycle checkpoint machinery in the absence of the MRX complex. This conclusion is further substantiated by the physical detection by ChIP of the Mre11 protein at the repeat tract. Therefore the MRX complex is likely acting as a sensor of damage at the repeat tract, interfacing with a signaling kinase such as Tel1 or Mec1. Our previous observation of increased CAG fragility in a *mec1Δ sml1Δ* strain of a similar magnitude to that observed in *mre11Δ*, whereas a *tel1Δ* did not increase CAG fragility, suggests that Mec1 is a good candidate for signaling from Mre11 bound damage [12,27]. An alternative interpretation is that MRX is needed to create the checkpoint signal, for example by exposing ssDNA that can be coated by RPA. However, our previous results showed that mutation of the Mre11 nuclease activity or associated Exo1 or Sae2 nucleases did not fully recapitulate the *mre11Δ* phenotype [12], suggesting that MRX has a function in addition to processing. Interestingly, the overall checkpoint response is not compromised in *mre11Δ* cells, as constitutive Rad53 phosphorylation was detected, and the CAG-0 arrest phenotypes also indicate a robust and intact global checkpoint response. The S-phase localization of Mre11p to the repeat and the reduced recovery of S phase arrests in the *mre11Δ* CAG-155 strain (Figure S4) suggest that the primary repeat-induced damage sensed by the MRX complex may arise during replication. Since Mre11p has also been found at HU stalled forks [40], it may be recognizing the double-strand end at either a reversed or broken fork. The consequences of the absence of MRX sensing are a large increase in CAG fragility, expansions, and cytotoxicity [12].

An interesting and unexpected finding was that the two repeat lengths, CAG-70 and CAG-155, did not behave identically, suggesting that there are some differences in the DNA structures eliciting the checkpoint at each repeat. Based on the relief of growth and arrest defects by deletion of *MRE11*, Mre11 appears to be the primary sensor of damage at CAG-70. In contrast, cells with a CAG-155 tract still showed some arrest phenotypes in *mre11Δ* cells, but were particularly dependent on Rad52 for normal growth. Based on these results and previous data that a

strain mutated for Mrc1 checkpoint function had a high rate of CAG-155 fragility, we speculate that the longer repeat is detected more efficiently by sensors of fork stalling, such as Mrc1, making it less dependent on signaling through the MRX complex. It may be that both repeats elicit fork reversal and occasional DSBs that are sensed by MRX, but that the CAG-155 repeat is also able to stall a replication fork long enough to elicit an Mrc1-dependent checkpoint signal. Intriguingly, despite a robust checkpoint response in CAG-155 cells as measured by Rad53 phosphorylation, they formed a slightly larger average microcolony size than cells with a CAG-70 tract. This could be either due to the greater tendency of the CAG-155 strain to adapt (Table 1), or due to the greater amount of cell swelling (Figure 3B), taking up more space in the microcolony. Perhaps the hypothesized better S-phase structure detection allows for a timelier repair process at the longer repeat.

Do other structure-forming sequences elicit similar checkpoint responses? Expanded CGG/CCG repeats, inverted repeats, and alternative DNA structures such as H-DNA and Z-DNA are hotspots of replication stalling, chromosome breakage and rearrangements, and thus might elicit a similar response [42]. Yet genetic data suggest that expanded CGG repeats may be less efficient at eliciting a checkpoint than CAG repeats, as fork arrest at a CGG repeat was not dependent on the checkpoint function of Mrc1 whereas suppression of CAG fragility and instability is [26,28,43]. On the other hand, mice with an expanded CGG repeat at the fragile X locus and heterozygous for ATR or ATM exhibit increased frequencies of repeat expansion during intergenerational transmission and in somatic cells [44-45], suggesting that there is some level of checkpoint response to expanded CGG repeats. Variables that could affect the response to different sequences include the nature of the initial damage, processing of the damage, the amount of exposed ssDNA, or the chromatin structure at the repeat. Paradoxically, the ability of CAG repeats to be efficiently recognized by the checkpoint machinery may be helpful in preventing some level of CAG fragility, which is recovered at a lower rate than fragility at expanded CGG/CCG repeats in yeast [46] and has not yet been detected at human disease loci. It will be informative to directly compare the checkpoint responses to CAG *versus* CGG repeats and other structure-forming sequences in the future.

What relevance might our results have for human repeat expansion diseases? It is known that the RNA and protein products of transcribed and translated CAG/CTG repeats can be toxic to cells. Now we provide the additional knowledge that the expanded DNA itself can be toxic through mechanisms involving DNA replication and DNA damage repair. Since sense or antisense transcription across repeats could contribute to structure formation [47], the baseline of repeat-induced cytotoxicity may be higher in instances where the CAG repeat locus is also heavily or convergently transcribed [39]. In a multi-cellular organism, many of the long and recurring arrests we observed would probably lead to apoptosis and cell death, the main cause of disease symptoms and morbidity. Indeed, checkpoint activation and cell cycle re-entry have been observed during apoptosis of aging brains of patients with Huntington's as well as other neurodegenerative diseases [48]. A second finding with potential relevance for repeat expansion diseases is that repeat expansions are more frequent in cells undergoing a checkpoint response. Intriguingly, re-entry into the cell cycle after DNA damage can facilitate repair in postmitotic neurons [49], which could possibly contribute to further repeat expansions. Therefore, DNA repair occurring in the context of an activated checkpoint response may be a cause of repeat expansions in mammalian cells as well.

## Materials and Methods

### Yeast strains, YAC, and media

YAC CF1 harboring CAG repeats is described in [12,29]. In this YAC, the CAG repeat is oriented such that the CAG strand is the lagging strand template (the more stable and expansion-prone orientation). For all experiments, yeast strains harboring YAC-CF1 with CAG repeats (CAG- 70, 155, or 195 repeats; Table S2) were plated onto YC-Ura-Leu solid media for single colonies and grown for 3 days at 30 °C. CAG repeat length from a portion of the colony was determined by colony PCR [29]. Starting colonies with intact tract lengths were chosen for experiments.

### Microcolony and single cell pedigree analyses

20  $\mu$ l of overnight culture ( $\sim$ 7.0 doublings) was spread as a stripe onto yeast complete solid media lacking Leucine (YC-Leu). Single unbudded, normal-sized G1 cells from the stripe were micromanipulated away to designated locations on the plate using a Nikon Eclipse E400 tetrad dissection scope. Precursor cells were allowed to divide for either 30 hours (microcolony experiment) or 18 hours (pedigree experiment) at 30 °C. For the microcolony experiment, the growth of precursor cells into microcolonies (small colonies) was recorded at 5-hour, 10-hour and 30-hour time intervals. An average of 40 cells (range 22–73) from two experiments were analyzed per strain. Pictures were taken at 10X magnification using an Olympus microscope, and microcolony area at 30 hours was measured using the National Institutes of Health (NIH) ImageJ software. Survivors (plotted) were defined as  $\text{area} \geq 0.01 \text{ mm}^2$ ; nonsurvivors (not shown) were defined as  $\text{area} \leq 0.005 \text{ mm}^2$  (cutoff values in [12] reported incorrectly and corrected here). The data set was subjected to non-linear regression analysis and graphed using the Prism curve-fitting software (GraphPad Software, San Diego, CA). Analysis of variance (ANOVA) was used to compare microcolony areas. Fisher's LSD post-hoc test was used to quantify growth differences among CAG -0, -70 and -155 repeat-containing strains within each genotype.

For single cell pedigree analysis, individual divisions within and across pedigrees were monitored for a duration of  $\sim$ 18 hours (5–7 divisions) on YC-Leu media at 30 °C. This number of divisions was chosen to minimize any confounding effects of senescence and allow a fair comparison between WT and DSB repair mutants that have a compromised division potential (see Text S1 for further information). 15–41 lineages were monitored in parallel on five plates for a total of 31–183 cell divisions; see Table S1 for raw numbers. Mother cells were followed as they do not have a size-related growth delay; daughter cells were discarded. As a rule, precursor cells that failed to initiate growth (increase in cell volume) or initiate division were excluded from the experiment since they could have been damaged during micromanipulation. The duration of individual cell division, i.e. growth from a single unbudded cell until separation into daughter cells was recorded; the duration of a normal yeast cell division was set at  $\leq$ 3.0 hours to factor in delays in division introduced by mechanical stress due to micromanipulation, observed to be 30–45 minutes. A bud to mother ratio of  $<$ 33% was deemed an S phase cell (small-medium bud), or  $>$ 33% a G2/M phase cell (large budded) [50]. Cell cycle position at the G1, S or G2/M phases was recorded at least twice within a division cycle. Elongated buds were typed as S phase arrests since they occurred after S phase onset. Multibuds were classified as G2/M arrests since they arose after G2 phase onset. Cells that were small budded when a cell cycle delay occurred were categorized as S phase “arrests”, although the S phase checkpoint does not result

in a true arrest, but a slowing of S phase and eventual entry into G2. Cell sizes greater than the size of a normal yeast cell ( $>$ 8  $\mu$ m diameter) were counted as swollen. Because of interdivisional variation in cell size, the G1 cell of each division was set as the normal size standard for that division, allowing for unbiased assessment of cell swelling among cell divisions. Pictures of swollen cells were taken using a Nikon D40 camera under 80X magnification. Cell area was measured by NIH ImageJ software. Results were graphed using MATLAB version 7.9 (R2009b) software (The Mathworks, Natick, MA).

### CAG repeat tract PCR

CAG-70 tracts were chosen to analyze, as expansions are more reliably detected for this length. For the HU experiment, overnight WT CAG-70 cultures were grown for  $\sim$ 7.0 doublings in YC-Leu liquid media  $\pm$  0.1 M HU, plated on YC-Leu solid media  $\pm$  0.1 M HU, and allowed to form daughter colonies at 30 °C for 3 days. Alternatively, single cells from an overnight YC-Leu culture were micromanipulated on to YC-Leu solid media, and grown for  $\sim$ 3 days until they attained maximal sizes. A partial normal-sized colony or entire poorly growing colony (defined as growing to one-third or less the size of a normal colony) was used for colony PCR using conditions described in [12]. In a subset of colonies showing partial instability, PCR amplification products  $>$ 10% or  $>$ 30% of the intensity of the intact band respectively, were counted as an expansion or contraction event.

### Fluorescence activated cell sorting (FACS) analysis to monitor cell cycle progression

Yeast strains were grown in 1 ml of YC-Leu liquid media with 2% glucose until late-log to early stationary phase. 1 ml of the culture ( $\sim$ 1  $\times$  10<sup>7</sup> cells) was pelleted, washed 3X with sterile water, resuspended in cold 70% (w/v) ethanol followed by overnight incubation at 4 °C. Cells were subsequently pelleted, resuspended in 50 mM Tris-HCl (pH 7.5) buffer containing 1 mg/ml RNaseA, followed by overnight incubation at 37 °C. FACS analysis samples were prepared by pretreatment with 55 mM HCl with 5 mg/ml pepsin, washed and resuspended in FACS buffer (200 mM Tris pH 7.5; 211 mM NaCl; 78 mM MgCl<sub>2</sub> adjusted to pH 7.5 with HCl) containing 1 mg/ml propidium iodide, incubated at  $-$ 20 °C for 1 hour, transferred to 1 ml of 50 mM Tris pH 7.5 and subjected to sonication. The total cellular DNA content from an average of 100,000 cells was measured using a FACS-Calibur flow cytometer and BD CellQuest software. FACS plots were generated using ModFit LT software.

### Immunoblotting to detect Rad53 phosphorylation in CAG repeat-containing cells

Total cellular protein was prepared using the trichloroacetic acid (TCA) method described in [51] for immunoblotting. Briefly,  $\sim$ 10<sup>8</sup> exponentially growing cells (as determined by OD<sub>600</sub> and hemocytometer counting) were pelleted, washed and resuspended in 20% TCA. Samples were vortexed with glass beads, pelleted at 3000 rpm, boiled in Laemmli buffer (BioRad) and the resulting extracts clarified by centrifugation at 3000 rpm. 15  $\mu$ g of total protein (quantified by Bradford method) was loaded per lane; proteins were resolved on an 8% SDS-polyacrylamide gel and transferred to a polyvinylidene difluoride membrane (GE Amersham). The membrane was blocked in 5% milk in TBS-T (Tween, 0.1%), incubated with polyclonal, Rad53 primary antibody (Santa Cruz Biotechnologies) followed by washes in TBS-T (0.1%) and incubation with secondary Anti-goat HRP antibody (Santa Cruz Biotechnologies). Phosphorylated isoforms

of Rad53 were visualized by chemiluminescence (Millipore). Semi-quantitative densitometry of phosphorylated Rad53 isoforms was performed using the NIH ImageJ software on film exposures where the signal fell within the linear range. Resultant values were graphed using MS Excel software.

### Chromatin immunoprecipitation (ChIP)

A strain with TAP-tagged Mre11 [52] and a CAG-155 repeat was used for ChIP. Yeast cultures grown to an OD<sub>600</sub> of 0.6 were either unsynchronized (Asynch) or synchronized in G1 with  $\alpha$ -factor, released into S phase, and samples collected at the indicated time points. Chromatin samples were cross-linked using formaldehyde and processed according to [53]. Mre11-TAP:DNA complexes were immunoprecipitated using rabbit IgG agarose beads directed against protein A on the TAP tag (Sigma) [52]. Real-time quantitative PCR was used to amplify a 150 bp fragment 186 bp proximal to the CAG repeat using CAGfor and CAGrev primers in IP and whole cell extract (WCE) fractions and an untagged control strain. Similarly, a non-repeat reference locus (*ACT1*) was amplified from IP, WCE and untagged control fractions (amplicon length 146 bp, amplified using Act1for2 and Act1rev2 primers; all primers available upon request).  $2^{-\Delta\Delta Ct}$  value, i.e. fold enrichment of Mre11-TAP at CAG repeat-containing DNA fragment was obtained by normalizing CAG locus amplification to *ACT1* locus amplification in IP and WCE samples. The untagged control showed no enrichment at the CAG locus over the *ACT1* locus ( $2^{-\Delta\Delta Ct}$  value of 1-fold). PCR was performed using SYBR-green PCR mix (BioRad) on an ABI Prism 7300 sequence detection system. Each PCR reaction was set up in triplicate; PCR cycling conditions- 95 °C for 3 min, 40 cycles of 95 °C for 15 s and 60 °C for 30 s. Asynch, 10 min and 20 min time points represent the average of 3, 3, and 4 independent experiments respectively; 0 and 40 min values derived from one experiment.

### Statistical analyses

Analysis of variance (ANOVA) with a three-way Fisher's LSD post-hoc test was used to compare microcolony areas. Doubling efficiency curves were analyzed using Wilcoxon's sum-rank test. Logistic regression analysis using Chi-square statistics was used to perform 3X2 comparisons on pedigree data sets to determine repeat-specific effects within genotypes; statistically significant ( $p < 0.05$ ) interactions were further subjected to a Wald's post-hoc test (see Table S1). A 2X2 Fisher's exact test was used to compare among genotypes to determine gene specific effects at each CAG repeat length. Analyses were performed using either SAS version 9.1 (SAS Inc. 2003) or SPSS Statistics GradPack Version 17.0, 2008 software.

### Supporting Information

**Figure S1** Repeat-containing cells show growth delays in liquid culture relative to a CAG-0 control strain. (A) and (B) represent growth curves of wild-type cells with expanded CAG-195 repeats or no-repeat control from two independent experiments. Note different X-axis intervals in graphs. Overnight cultures were diluted to a starting OD<sub>600</sub> of ~0.04 in YC-Leu liquid media and grown at 30 °C for up to 72 hours. Growth was periodically

measured using a spectrophotometer (Eppendorf) and viability is represented as optical density units (OD<sub>600</sub>) plotted against time. Found at: doi:10.1371/journal.pgen.1001339.s001 (0.07 MB TIF)

**Figure S2** Cells with expanded CAG-70 or CAG-155 repeats experience protracted cell division cycles. (A) Wild-type, (B, C, D) DSB repair-deficient backgrounds. Graphs represent percent of divisions observed for each time window; sample size mean is 86 divisions; range of 31–183 divisions; Table S1. Data points include divisions that have completed and end divisions with indeterminate end points. Found at: doi:10.1371/journal.pgen.1001339.s002 (0.14 MB TIF)

**Figure S3** Replication stress leads to cell swelling in S and G2 phases as well as multibudded morphology. The WT CAG-0 strain was grown in YC-Leu liquid media in the presence of 0.1 M HU for 16 hours (a sub-lethal dose that causes replication stress but not full arrest); cells were classified as G1, S, G2/M or multibudded based on budding index. Numbers on graph represent data from two independent experiments; sample size scored for each treatment = 784 cells (–HU), 401 cells (+HU). \* represents  $p < 0.01$  by Fisher's exact test. Found at: doi:10.1371/journal.pgen.1001339.s003 (0.06 MB TIF)

**Figure S4** Cell cycle position of arrests in *mre11Δ* and *dnl1Δ* strains. Cell cycle position of arrests (>3.0 hrs) observed for cells dividing on YC-Leu solid media in the single cell pedigree analysis. Arrests defined as >60' for G1, >45' for S, >60' for G2/M. Not included are normal divisions <3.0 hours that show an occasional S phase or G2/M delay. Statistically significant comparisons to CAG-0 (\*) or between CAG-70 and CAG-155 strains (†) within genotype are indicated. Statistics performed by logistic regression analysis on raw data calculated out of total number of divisions (Table S1). Found at: doi:10.1371/journal.pgen.1001339.s004 (0.17 MB TIF)

**Table S1** Raw Numbers from Pedigree Analysis, with p-values. Found at: doi:10.1371/journal.pgen.1001339.s005 (0.17 MB DOC)

**Table S2** List of yeast strains used in the study. Found at: doi:10.1371/journal.pgen.1001339.s006 (0.13 MB DOC)

**Text S1** Differences between DNA damage checkpoint response and cellular senescences. Found at: doi:10.1371/journal.pgen.1001339.s007 (0.02 MB DOC)

### Acknowledgments

We thank Michael Reed and Durwood Marshall for help with statistical analyses of the microcolony and pedigree data sets, Sara Lewis and Randi Rotjan for statistics discussions, Minda Berbeco for help with SPSS software, Melissa Koch and Jiahui Yang for RT-PCR analysis, Nevan Krogan for the Mre11-TAP tagged strain, and the Tufts CORE facility for FACS analysis.

### Author Contributions

Conceived and designed the experiments: RS CHF. Performed the experiments: RS. Analyzed the data: RS CHF. Wrote the paper: RS CHF.

### References

- Richard GF, Kerrest A, Dujon B (2008) Comparative genomics and molecular dynamics of DNA repeats in eukaryotes. *Microbiol Mol Biol Rev* 72: 686–727.
- Orr HT, Zoghbi HY (2007) Trinucleotide repeat disorders. *Annu Rev Neurosci* 30: 575–621.
- Brouwer JR, Willemsen R, Oostra BA (2009) Microsatellite repeat instability and neurological disease. *Bioessays* 31: 71–83.
- Mirkin SM (2007) Expandable DNA repeats and human disease. *Nature* 447: 932–940.



5. Samadashwily GM, Raca G, Mirkin SM (1997) Trinucleotide repeats affect DNA replication in vivo. *Nat Genet* 17: 298–304.
6. Pelletier R, Krasilnikova MM, Samadashwily GM, Lahue R, Mirkin SM (2003) Replication and expansion of trinucleotide repeats in yeast. *Mol Cell Biol* 23: 1349–1357.
7. Kerrest A, Anand RP, Sundararajan R, Bermejo R, Liberi G, et al. (2009) SRS2 and SGS1 prevent chromosomal breaks and stabilize triplet repeats by restraining recombination. *Nat Struct Mol Biol* 16: 159–167.
8. Liu Y, Kao HI, Bambara RA (2004) Flap endonuclease 1: a central component of DNA metabolism. *Annu Rev Biochem* 73: 589–615.
9. Panigrahi GB, Lau R, Montgomery SE, Leonard MR, Pearson CE (2005) Slipped (CTG)<sub>n</sub>(CAG) repeats can be correctly repaired, escape repair or undergo error-prone repair. *Nat Struct Mol Biol* 12: 654–662.
10. Freudenreich CH (2007) Chromosome fragility: molecular mechanisms and cellular consequences. *Front Biosci* 12: 4911–4924.
11. Kim HM, Narayanan V, Mieczkowski PA, Petes TD, Krasilnikova MM, et al. (2008) Chromosome fragility at GAA tracts in yeast depends on repeat orientation and requires mismatch repair. *EMBO J* 27: 2896–2906.
12. Sundararajan R, Gellon L, Zunder RM, Freudenreich CH (2010) Double-strand break repair pathways protect against CAG/CTG repeat expansions, contractions and repeat-mediated chromosomal fragility in *Saccharomyces cerevisiae*. *Genetics* 184: 65–77.
13. Krogh BO, Symington LS (2004) Recombination proteins in yeast. *Annu Rev Genet* 38: 233–271.
14. Lisby M, Rothstein R (2009) Choreography of recombination proteins during the DNA damage response. *DNA Repair (Amst)* 8: 1068–1076.
15. Sogo JM, Lopes M, Foiani M (2002) Fork reversal and ssDNA accumulation at stalled replication forks owing to checkpoint defects. *Science* 297: 599–602.
16. Harrison JC, Haber JE (2006) Surviving the breakup: the DNA damage checkpoint. *Annu Rev Genet* 40: 209–235.
17. Putnam CD, Jaehnig EJ, Kolodner RD (2009) Perspectives on the DNA damage and replication checkpoint responses in *Saccharomyces cerevisiae*. *DNA Repair (Amst)* 8: 974–982.
18. Paulovich AG, Hartwell LH (1995) A checkpoint regulates the rate of progression through S phase in *S. cerevisiae* in response to DNA damage. *Cell* 82: 841–847.
19. Lopes M, Cotta-Ramusino C, Pellicoli A, Liberi G, Plevani P, et al. (2001) The DNA replication checkpoint response stabilizes stalled replication forks. *Nature* 412: 557–561.
20. Redon C, Pilch DR, Rogakou EP, Orr AH, Lowndes NF, et al. (2003) Yeast histone 2A serine 129 is essential for the efficient repair of checkpoint-blind DNA damage. *EMBO Rep* 4: 678–684.
21. Sandell LL, Zakian VA (1993) Loss of a yeast telomere: arrest, recovery, and chromosome loss. *Cell* 75: 729–739.
22. Toczyski DP, Galgoczy DJ, Hartwell LH (1997) CDC5 and CKII control adaptation to the yeast DNA damage checkpoint. *Cell* 90: 1097–1106.
23. Clemenson C, Marsolier-Kergoat MC (2009) DNA damage checkpoint inactivation: adaptation and recovery. *DNA Repair (Amst)* 8: 1101–1109.
24. Khanna KK, Jackson SP (2001) DNA double-strand breaks: signaling, repair and the cancer connection. *Nat Genet* 27: 247–254.
25. Castedo M, Perfettini JL, Roumier T, Andreau K, Medema R, et al. (2004) Cell death by mitotic catastrophe: a molecular definition. *Oncogene* 23: 2825–2837.
26. Freudenreich CH, Lahiri M (2004) Structure-forming CAG/CTG repeat sequences are sensitive to breakage in the absence of Mre1 checkpoint function and S-phase checkpoint signaling: implications for trinucleotide repeat expansion diseases. *Cell Cycle* 3: 1370–1374.
27. Lahiri M, Gustafson TL, Majors ER, Freudenreich CH (2004) Expanded CAG repeats activate the DNA damage checkpoint pathway. *Mol Cell* 15: 287–293.
28. Razioldo DF, Lahue RS (2008) Mre1, Tof1 and Csm3 inhibit CAG/CTG repeat instability by at least two mechanisms. *DNA Repair (Amst)* 7: 633–640.
29. Callahan JL, Andrews KJ, Zakian VA, Freudenreich CH (2003) Mutations in yeast replication proteins that increase CAG/CTG expansions also increase repeat fragility. *Mol Cell Biol* 23: 7849–7860.
30. Bowater RP, Rosche WA, Jaworski A, Sinden RR, Wells RD (1996) Relationship between *Escherichia coli* growth and deletions of CTG/CAG triplet repeats in plasmids. *J Mol Biol* 264: 82–96.
31. Weinert TA, Hartwell LH (1988) The RAD9 gene controls the cell cycle response to DNA damage in *Saccharomyces cerevisiae*. *Science* 241: 317–322.
32. Lee SE, Moore JK, Holmes A, Umez K, Kolodner RD, et al. (1998) *Saccharomyces Ku70*, *mre11/rad50* and RPA proteins regulate adaptation to G2/M arrest after DNA damage. *Cell* 94: 399–409.
33. Petrini JH, Stracker TH (2003) The cellular response to DNA double-strand breaks: defining the sensors and mediators. *Trends Cell Biol* 13: 458–462.
34. Vaze MB, Pellicoli A, Lee SE, Ira G, Liberi G, et al. (2002) Recovery from checkpoint-mediated arrest after repair of a double-strand break requires Srs2 helicase. *Mol Cell* 10: 373–385.
35. Hartwell LH, Culotti J, Pringle JR, Reid BJ (1974) Genetic control of the cell division cycle in yeast. *Science* 183: 46–51.
36. Enserink JM, Smolka MB, Zhou H, Kolodner RD (2006) Checkpoint proteins control morphogenetic events during DNA replication stress in *Saccharomyces cerevisiae*. *J Cell Biol* 175: 729–741.
37. Jiang YW, Kang CM (2003) Induction of *S. cerevisiae* filamentous differentiation by slowed DNA synthesis involves Mec1, Rad53 and Swe1 checkpoint proteins. *Mol Biol Cell* 14: 5116–5124.
38. Freudenreich CH, Kantrow SM, Zakian VA (1998) Expansion and length-dependent fragility of CTG repeats in yeast. *Science* 279: 853–856.
39. Lin Y, Leng M, Wan M, Wilson JH (2010) Convergent Transcription through a Long CAG Tract Destabilizes Repeats and Induces Apoptosis. *Mol Cell Biol*.
40. Tittel-Elmer M, Alabert C, Pasero P, Cobb JA (2009) The MRX complex stabilizes the replisome independently of the S phase checkpoint during replication stress. *EMBO J* 28: 1142–1156.
41. Kuzminov A (2001) DNA replication meets genetic exchange: chromosomal damage and its repair by homologous recombination. *Proc Natl Acad Sci U S A* 98: 8461–8468.
42. Voineagu I, Freudenreich CH, Mirkin SM (2009) Checkpoint responses to unusual structures formed by DNA repeats. *Mol Carcinog* 48: 309–318.
43. Voineagu I, Surka CF, Shishkin AA, Krasilnikova MM, Mirkin SM (2009) Replisome stalling and stabilization at CGG repeats, which are responsible for chromosomal fragility. *Nat Struct Mol Biol* 16: 226–228.
44. Entezam A, Usdin K (2009) ATM and ATR protect the genome against two different types of tandem repeat instability in Fragile X premutation mice. *Nucleic Acids Res* 37: 6371–6377.
45. Entezam A, Usdin K (2008) ATR protects the genome against CGG/CCG-repeat expansion in Fragile X premutation mice. *Nucleic Acids Res* 36: 1050–1056.
46. Balakumaran BS, Freudenreich CH, Zakian VA (2000) CGG/CCG repeats exhibit orientation-dependent instability and orientation-independent fragility in *Saccharomyces cerevisiae*. *Hum Mol Genet* 9: 93–100.
47. Lin Y, Dion V, Wilson JH (2006) Transcription promotes contraction of CAG repeat tracts in human cells. *Nat Struct Mol Biol* 13: 179–180.
48. Kruman II, Schwartz EI (2008) DNA damage response and neuroprotection. *Front Biosci* 13: 2504–2515.
49. Schwartz EI, Smilenov LB, Price MA, Osredkar T, Baker RA, et al. (2007) Cell cycle activation in postmitotic neurons is essential for DNA repair. *Cell Cycle* 6: 318–329.
50. Lisby M, Barlow JH, Burgess RC, Rothstein R (2004) Choreography of the DNA damage response: spatiotemporal relationships among checkpoint and repair proteins. *Cell* 118: 699–713.
51. Foiani M, Ferrari M, Liberi G, Lopes M, Lucca C, et al. (1998) S-phase DNA damage checkpoint in budding yeast. *Biol Chem* 379: 1019–1023.
52. Krogan NJ, Kim M, Tong A, Golshani A, Cagney G, et al. (2003) Methylation of histone H3 by Set2 in *Saccharomyces cerevisiae* is linked to transcriptional elongation by RNA polymerase II. *Mol Cell Biol* 23: 4207–4218.
53. Aparicio O, Geisberg JV, Sekinger E, Yang A, Moqtaderi Z, et al. (2005) Chromatin immunoprecipitation for determining the association of proteins with specific genomic sequences in vivo. *Curr Protoc Mol Biol* Chapter 21: Unit 21 23.